

# **Formation and fate of carboxylic acids in the lignin-first biorefining of lignocellulose via H-transfer catalyzed by Raney Ni**

Inês Graça,<sup>a</sup> Robert T. Woodward,<sup>a</sup> Marco Kennema,<sup>b</sup> Roberto Rinaldi<sup>a,\*</sup>

<sup>a</sup> Imperial College London, Department of Chemical Engineering, South Kensington Campus,  
SW7 2AZ London, United Kingdom

<sup>b</sup> Max-Planck-Institut für Kohlenforschung, Kaiser-Wilhelm-Platz 1, D- 45470 Mülheim an  
der Ruhr, Germany

\* Corresponding author: R. Rinaldi, [rrinaldi@imperial.ac.uk](mailto:rrinaldi@imperial.ac.uk)

*Keywords: Lignin-first biorefining, carboxylic acid, Raney Ni, catalyst stability, catalytic H-transfer, 2-propanol*

## Abstract

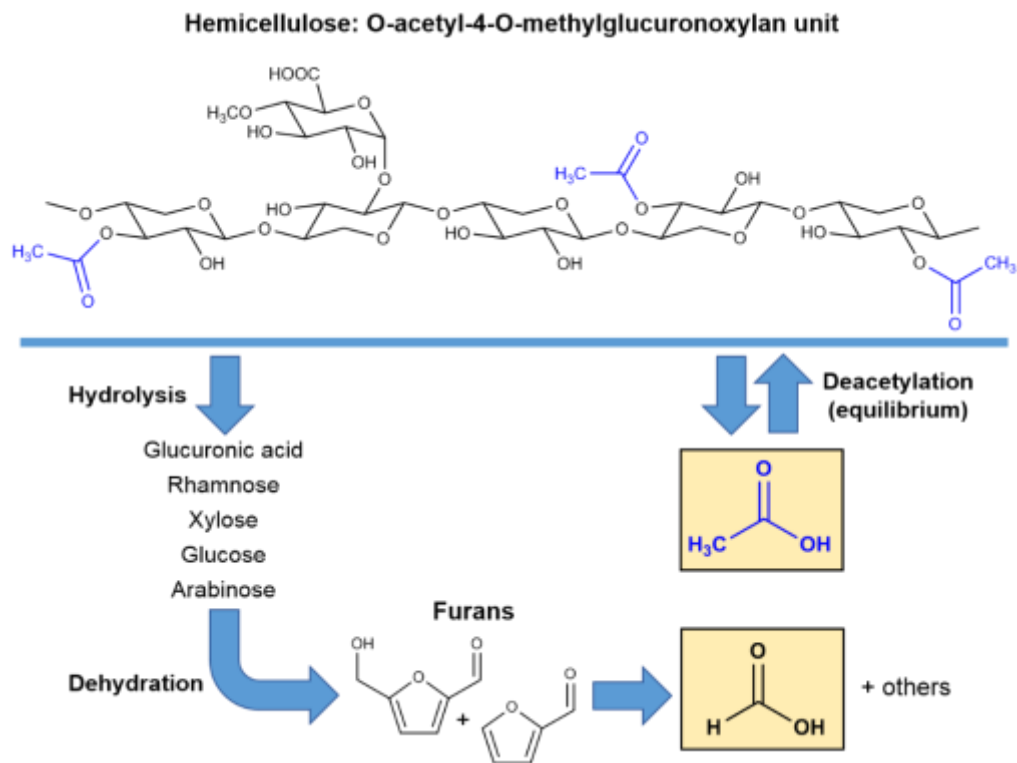
Lignin-first biorefining constitutes a new research field in which the overarching objective is the prevention of lignin recalcitrance while providing high-quality pulps. For this purpose, the solvent extraction of lignin is performed in the presence of a hydrogenation catalyst, employing H<sub>2</sub> pressure or an H-donor solvent (e.g. 2-propanol), and thus leading to passivation of reactive lignin fragments *via* reductive processes. As a result, lignin-first biorefining methods generate high-quality pulps in addition to low-molecular-weight lignin streams with high molecular uniformity. Nonetheless, upon cooking lignocellulose in solvent mixtures containing water, other processes on the lignocellulosic matrix take place, releasing soluble intermediates. In fact, hemicellulose undergoes deacetylation, to a variable extent, releasing acetic acid into the liquor. Moreover, formic acid can also be formed as a degradation product of hemicellulose C<sub>6</sub>-sugars also released into the liquor. However, despite this general notion, the formation and fate of these carboxylic acids during the cooking of lignocellulosic substrates, and the effects these acids may have on hydrogenation catalyst performance remain poorly understood. In this report, we examine both the formation and subsequent fate of formic acid and acetic acid during lignocellulose deconstruction for both a lignin-first biorefining method (via H-transfer reactions in the presence of Raney Ni catalyst) and its equivalent Organosolv process with no added acid or hydrogenation catalyst. An apparent mechanism for the mitigation of formic acid formation in the presence of Raney Ni catalyst is outlined *via* the hydrogenation of sugars to sugar alcohols. Furthermore, the effects of the carboxylic acids on Raney Ni performance are assessed, using the transfer-hydrogenation of phenol to cyclohexanol/cyclohexanone as a model reaction, elucidating inhibition rates of the acids. Finally, we conclude with the implications of these results for the design of lignin-first biorefining processes. In a broader context, understanding of the formation and fate of carboxylic acids during CUB is crucial to producing high-quality pulps with high degrees of polymerization and high xylan contents.

## Introduction

Catalytic Upstream Biorefining (CUB) or lignin-first biorefining represents a rapidly growing research area within the field of lignin valorization.<sup>(1)-(6)</sup> In CUB processes, also known as reductive catalytic fractionation, a hydrogenation catalyst is employed for the early-stage conversion of lignin fragments released upon cooking lignocellulose in water/organic solvent mixtures.<sup>(2),(4),(6)</sup> This strategy brings about the hydrodeoxygenation of reactive intermediates (i.e. Hibbert ketones and their degradation products), which constitutes an atom-economic way of suppressing re-condensation reactions often occurring in Organosolv and other stoichiometric pulping processes.<sup>(2),(4)</sup> Typically, CUB processes isolate lignin as a viscous oil along with delignified pulps. By varying the hydrogenation catalyst and solvent, the process can lead to different types of monophenolics as major components in lignin oil composition (e.g. 4-dihydro-*p*-monolignols, monolignols or alkyl(di)methoxyphenols) along with other minor products, such as lignin dimers, oligomers and polyols derived from the transformation of hemicellulose sugars released together with the lignin fragments).<sup>(1)-(12)</sup>

In 2014, we reported a CUB process based on the early-stage catalytic conversion of lignin (ECCL) *via* H-transfer reactions in the presence of Raney Ni.<sup>(7),(13)</sup> This process led to the selective hydrodeoxygenation of lignin fragment's propyl-side chains, resulting in much simpler mixtures of products in comparison to conventional methods for late-stage catalytic conversion of isolated technical lignins.<sup>(2)</sup> Noteworthy, lignin-first does not imply "cellulose-second". Recently, it was demonstrated that the CUB process in the presence of Raney Ni and 2-PrOH/H<sub>2</sub>O (7:3, v/v) produces holocellulosic pulps with larger degrees of polymerization and higher xylan contents, than pulps produced by Organosolv processes (with no added catalyst) under similar conditions.<sup>(13)</sup> It was put forward that these features are associated with

the higher pH of CUB liquors compared to those from the Organosolv process ( $\Delta\text{pH} = 1\text{-}2$ ), suggesting that Raney Ni should be able to decompose acidic content in the liquor by reductive processes,<sup>(7),(13)</sup> mostly in the form of acetic acid and formic acid.<sup>(6),(7),(14)-(19)</sup> Acetic acid is produced *via* the hydrolysis of the acetyl groups (*deacetylation*) of hemicellulose. The concentration of acetic acid is especially significant in the hydrolysates of hardwoods as O-acetyl groups substitute a considerable number of the OH-groups of the xylose units.<sup>(18),(20),(21)</sup> Indeed, acetyl groups account for 3-5% of hardwood's composition, while this number is 1-2% in softwoods.<sup>(21)</sup> On the other hand, formyl groups rarely occur in woods. Typically, formyl contents do not exceed 0.04% of the wood composition.<sup>(21)</sup> It is generally accepted that formic acid found in the liquors after lignin-extraction by an organic solvent (i.e. Organosolv processes) is primarily produced in the degradation of hemicellulose sugars formed by hemicellulose hydrolysis under cooking conditions.<sup>(18),(20),(21)</sup> In acidic medium, released saccharides (arabinose, glucose, xylose, rhamnose and galacturonic acid in Poplar wood)<sup>(22)</sup> undergo dehydration to forming furanic compounds, which may be further degraded to yield, for instance, formic acid in addition to levulinic acid.<sup>(18),(20),(23)-(26)</sup> Scheme 1 illustrates possible reactions leading to the formation and release of carboxylic acids into the liquor.



**Scheme 1.** Schematic representation of reactions leading to formic acid and acetic acid release upon the cooking of lignocellulosic biomass.

Despite some evidence indicating decreased carboxylic acid content in the CUB liquor, there is a knowledge gap in both the formation and fate of carboxylic acids in the lignin-first deconstruction of lignocellulosic biomass. Herein, a fundamental study on the formation and fate of acetic acid and formic acid from Poplar wood is presented. In order to shed light on the fate of these acids, a detailed analysis of the interaction between formic acid or acetic acid and the surface of Raney Ni, under conditions comparable to those of a CUB process, is performed. This report is organized as follows. Firstly, the evolution of acetic acid and formic acid levels in the CUB and Organosolv processes are compared. A mechanism underlining the mitigation of formic acid formation is presented in addition to the reactivity of carboxylic acids in the presence of Raney Ni. After which, the impact of formic acid and

acetic acid on the transfer-hydrogenation of phenol is assessed by pulse injection of the carboxylic acids into a continuously stirred tank reactor (CSTR) at 140 °C. The H-transfer of phenol was selected as a model reaction owing to its favorable kinetics in batch reactions and high selectivity for single products.<sup>(27),(28)</sup> To identify the main species interacting with Raney Ni upon adsorption of acetic acid and formic acid, the liquid-solid interface of Raney Ni was analyzed by surface attenuated total reflection infrared (ATR-IR) spectroscopy. Additionally, further understanding of the extent of the inhibition effect caused by the carboxylic acids on Raney Ni is provided through the analysis of the catalyst oxidation by Ni K-edge X-Ray absorption near-edge spectroscopy (Ni K-edge XANES). Finally, to investigate the inhibitory effect of carboxylic acids under conditions near to those of CUB process, the pulse injection experiments of H-transfer hydrogenation of phenol were performed at several temperatures. The results extrapolated to the lowest operating temperature of the CUB process (180 °C) indicate that the carboxylic acids play a marginal role in the Raney Ni performance under “real world” CUB conditions. Overall, this paper provides detailed fundamental knowledge on the impact of the presence of carboxylic acids on Raney Ni and their reactivity under conditions similar to the CUB process.

## **Results and Discussion**

### *Monitoring formic acid and acetic acid in the CUB and Organosolv liquor*

To examine the formation and fate of formic acid and acetic acid throughout both CUB and Organosolv processes (performed in 7:3 (v/v) 2-PrOH/H<sub>2</sub>O liquor at 200°C), the liquors were analyzed by LC-MS operating in Selected Ion Monitoring (SIM) mode. Compared in Figure

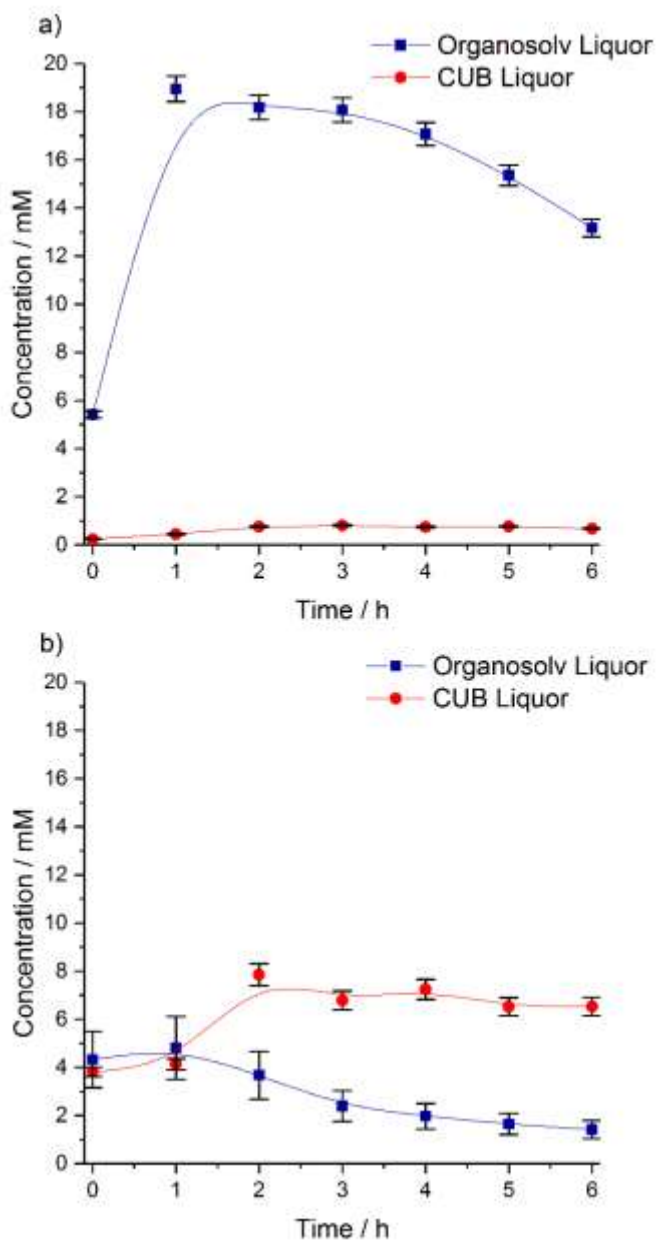
1 are the levels of formic acid and acetic acid released throughout the course of both CUB and Organosolv processes.

Figure 1 reveals key features of the chemistry of formic acid and acetic acid in both CUB and Organosolv liquors. Throughout both experiments, the levels of formic acid in the CUB liquor were markedly lower than those found in the Organosolv liquor (Figure 1a). At first sight, this observation might suggest formic acid is utilized as an H-source in the presence of Raney Ni. As it will be presented in the next section, this working hypothesis is, however, not entirely valid. The overall lower carboxylic acid levels measured in the CUB process in Figure 1 are in good agreement with the resulting pulp compositions for both the CUB and Organosolv processes (Table 1), as already reported by us.<sup>7,13</sup> Notably, xylan retention was improved in CUB derived pulps, in good agreement with a positive effect, expected from reduced acid concentrations, on the inhibition of hydrolysis of hemicellulose. Additionally, the presence of Raney Ni contributed to an increased delignification from 73 % (Organosolv process) to 80 % (CUB process).

**Table 1.** Weight yields of isolated fractions, pulp composition, and delignification extent obtained for Organosolv and CUB processes under identical process conditions.<sup>[a]</sup>

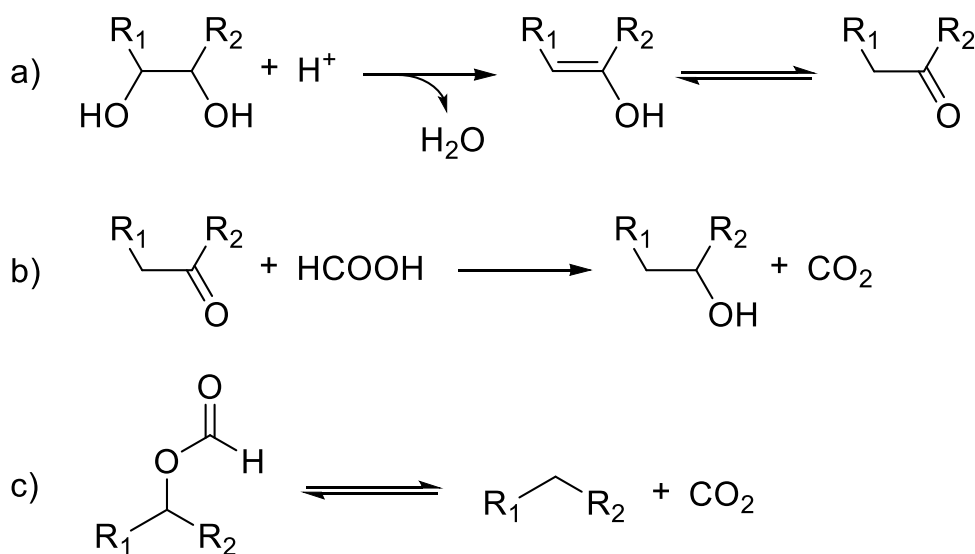
| Process type | Isolated fractions<br>/% relative to initial<br>substrate weight |      | Pulp composition <sup>[b],[c]</sup><br>/wt% |        |        |                       | Delignification<br>/% |
|--------------|--|------|---|--------|--------|-----------------------|-----------------------|
|              | Soluble  | Pulp | Glucans                                     | Xylans | Lignin | Others <sup>[d]</sup> |                       |
| Organosolv   | 33   | 53   | 79  | 6      | 8      | 7                     | 73                    |
| CUB          | 22   | 55   | 80  | 9      | 6      | 5                     | 80                    |

[a] General experimental conditions: Poplar wood (16.5 g), solvent (2 propanol:water, 7:3 v/v, 140 mL), 200 °C, 3h. CUB experiment was performed with the addition of Raney Ni (wet, 10 g); [b] Obtained from analytical saccharification with sulfuric acid; [c] Unprocessed Poplar wood composition: glucans 52 wt%, xylans 17 wt%, lignin 30 wt%, others 1 wt% (dry and ash-free values). [d] As part of the unidentified other products, acid-soluble lignin can comprise ~5 wt% of Poplar.



**Figure 1.** LC-MS (SIM mode) monitoring of the levels of (a) formic acid and (b) acetic acid in Organosolv and CUB liquors. Experimental conditions: 1) CUB: Poplar wood (17 g), wet Raney Ni (10 g), 2-propanol-water solution (7:3 v/v, 140 mL, as lignin-extracting liquor and H-donor), 200 °C; 2) Organosolv process: the experiment was carried out in the absence of Raney Ni under identical conditions to the CUB. Note that time measurement began upon the liquor reaching a temperature of 200 °C (ca. 60 min ramp time).

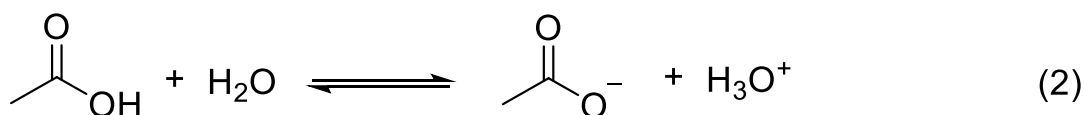
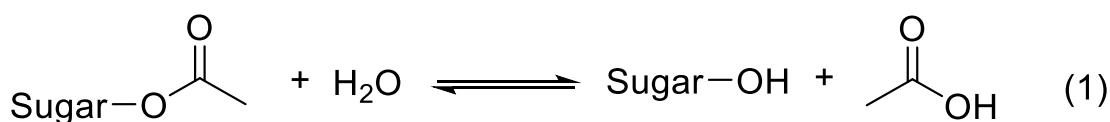
A less obvious trend is found for the evolution of formic acid in the Organosolv liquor (Figure 1a). This liquor showed a marked increase in formic acid concentration, from 5.4 to 18.9 mM, in the initial hour of Poplar wood cooking, after which, the formic acid levels gradually decreased to 13.2 mM at 6 h. This result suggests that formic acid is also utilized as a reducing agent in the Organosolv process. Previous works on hydrogenolysis of lignocellulosic substrates in the presence of formate/formic acid elucidated this route of formic acid consumption (Scheme 2a-c).<sup>(32)</sup> This process involves the formylation of hydroxyl groups occurring in sugars and lignin, followed by the elimination of CO<sub>2</sub>, leading to species hydrodeoxygenation.



**Scheme 2.** Hydrodeoxygenation of alcohol moieties occurring in sugars and lignin *via* formylation and CO<sub>2</sub> elimination.<sup>(32)</sup>

Regarding the formation of acetic acid, Figure 1b shows that, after 1h cooking of Poplar at 200°C, the levels of acetic acid in the CUB liquor became higher than those in the Organosolv liquor. Surprisingly, acetic acid levels decreased throughout the course of the

Organosolv process, while maintaining at a much higher concentration in the CUB liquor. As will be presented in the next section, Raney Ni is incapable of decomposing acetic acid *via* H-transfer reactions under CUB conditions. This new finding rejects, therefore, our previous hypothesis that the higher pH values of CUB liquor in comparison to those of the Organosolv liquor would be caused by the decomposition of acetic acid by Raney Ni.<sup>(7),(13)</sup> Accordingly, we propose here another working hypothesis: *the levels of formic acid in the liquor affects the extent of reversible deacetylation of hemicelluloses owing to their influence in the acid-base chemical equilibria in the process.* To investigate this hypothesis, we considered the chemical equilibrium involved in the deacetylation of hemicellulose and acetic acid/acetate equilibrium, as defined by (1) and (2), respectively:



As formic acid ( $\text{pK}_a = 3.75$ ) acidifies the liquors, the equilibrium (2) will shift to the left-hand side, increasing the levels of free acetic acid ( $\text{pK}_a = 4.8$ ). In turn, equilibrium (1) will respond to the resulting higher levels of free acetic acid, decreasing the extent of hemicellulose deacetylation. As a result, low levels of acetic acid should be found when the concentration of formic acid is increased.

To assess whether there is a relationship between the extent of deacetylation and the concentration of formic acid occurring in the liquor, we chose to examine the effect of formic

acid on the deacetylation of insoluble cellulose acetate as a model for the less-defined acetylated hemicelluloses. In this experiment, cellulose acetate was cooked at 200 °C with added formic acid in 2-PrOH/H<sub>2</sub>O (7:3, v/v). A control experiment was also performed in which no formic acid was added. The evolution of the levels of acetic acid and formic acid over cooking time was monitored by LC-MS operating in SIM mode. Figure 2a compares the evolution of acetic acid levels in the liquors in both the presence and absence of formic acid. In turn, in Figure 2b the concentration of formic acid is monitored with time in the experiment with added formic acid.

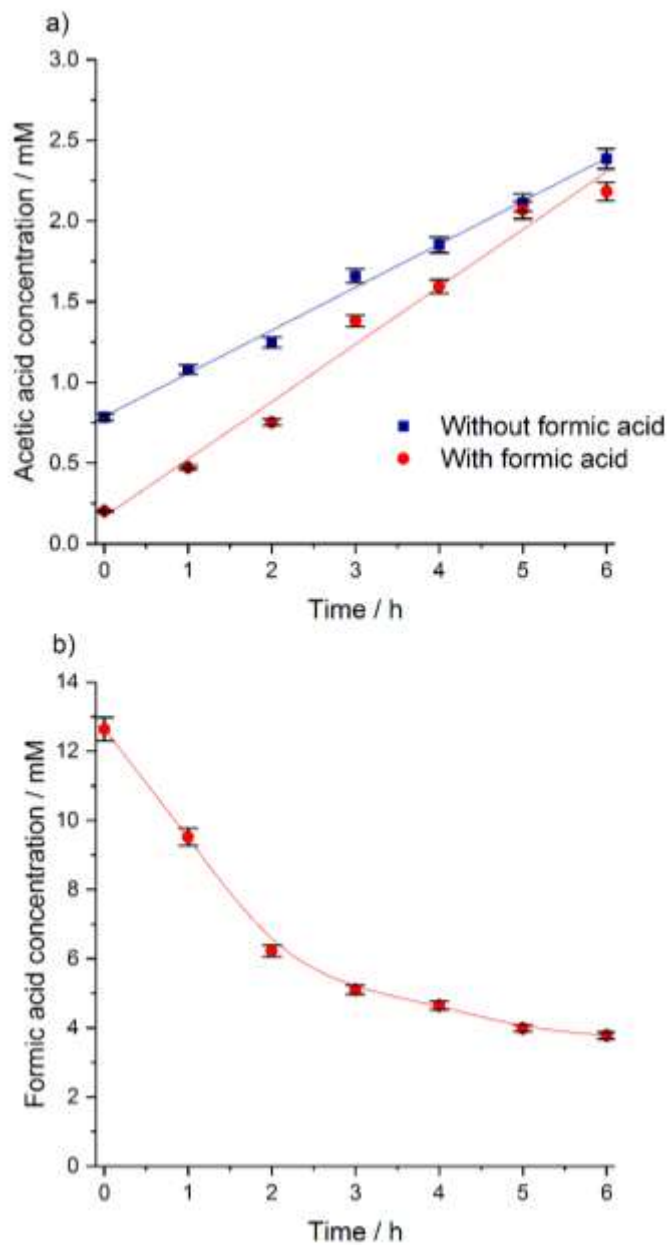


**Figure 2.** Deacetylation of cellulose acetate as a model reaction for understanding the effect of formic acid on the equilibrium of hemicellulose deacetylation: a) acetic acid concentration over time in experiments carried out with and without added formic acid; b) Monitoring of formic acid concentration with time in the experiment performed with added formic acid. Experimental conditions: cellulose acetate (0.25 g), 2-propanol-water solution (7:3 v/v, 140 mL), formic acid (15 mM), 200 °C. Note that time measurement began upon the liquor reaching a temperature of 200 °C (ca. 60 min ramp time, corresponding to a decrease in formic acid concentration from 15 to 12.6 mM).

Figure 2a shows that, in the initial 2 h of cooking of acetylated cellulose in the presence of formic acid, the acetic acid levels were considerably lower than those of the control experiment (i.e. no added formic acid). After 2 h, the acetic acid levels in both liquors started converging to around 2 mM. Notably, the convergence seems to be also associated with the considerable decay of formic acid concentration throughout the course of the experiment (Figure 2b). The concentration of formic acid (initial: 15 mM, which had decreased to 12.6 mM after the temperature ramping to 200 °C) decreased in the initial three hours of experiment, plateauing at about 4 mM at 4 h. As discussed previously, formic acid may also be consumed by reductive processes beginning with the formylation of free-alcohol groups. Most importantly, the data from Figure 2 supports the working hypothesis that high levels of formic acid in the liquor reduces the extent of deacetylation of hemicellulose as a response of the acid impact on the chemical equilibria (1) and (2). In fact, Gosselink *et al.*<sup>(21)</sup> reported that the addition of NaOH slightly increased the release of acetic acid when measuring acetyl and formyl group contents in fiber hemp by saponification in a mixture of 2-propanol/water. This concentration increase suggested that a medium of higher pH was favorable for deacetylation. In another paper, Kapu *et al.*<sup>(33)</sup> developed a mathematical model to predict  $\text{H}_3\text{O}^+$  evolution during autohydrolysis and dilute-acid hydrolysis of hemicellulose, considering all the processes governing  $\text{H}_3\text{O}^+$  concentration in solution (hydrolysis, deacetylation, equilibrium created by water dissociation, acid neutralization and addition of an external acid). The authors reported that the model predicts a steady-state  $\text{H}_3\text{O}^+$  concentration that depends on the equilibrium between the initial acetyl groups and added acid. Therefore, our results are in line with the previous observations that the deacetylation of hemicellulose is governed by the  $\text{H}_3\text{O}^+$  concentration in the liquors.<sup>(21),(33)</sup>

*Formation of formic acid and the reactivity of carboxylic acids in the presence of Raney Ni*

As revealed in Figure 1, a primary feature distinguishing CUB from Organosolv process is the low levels of formic acid present in the CUB liquor. In this section, the mechanisms underlining the occurrence of formic acid in low concentrations in the CUB liquor is presented. It has been demonstrated that Raney Ni/2-PrOH catalytic systems can quickly reduce the C<sub>5</sub>/C<sub>6</sub> sugars to the corresponding sugar alcohols.<sup>(1),(29)-(31)</sup> Building on those results, it is apparent that an alternate pathway resulting in the low concentrations of formic acid in the CUB liquor should be the hydrogenation of hemicellulose sugars. In fact, this reaction suppresses the formation of HMF and other furanic compounds, thus stopping the pathways for the formation of formic acid via hemicellulose sugars degradation. To verify this alternate pathway, the levels of C<sub>5</sub>/C<sub>6</sub> sugars and sugar alcohols in the liquors were also monitored using LC-MS operating in SIM mode. Figure 3 shows the evolution of the concentrations of sugars and sugar alcohols in the Organosolv and CUB liquors.

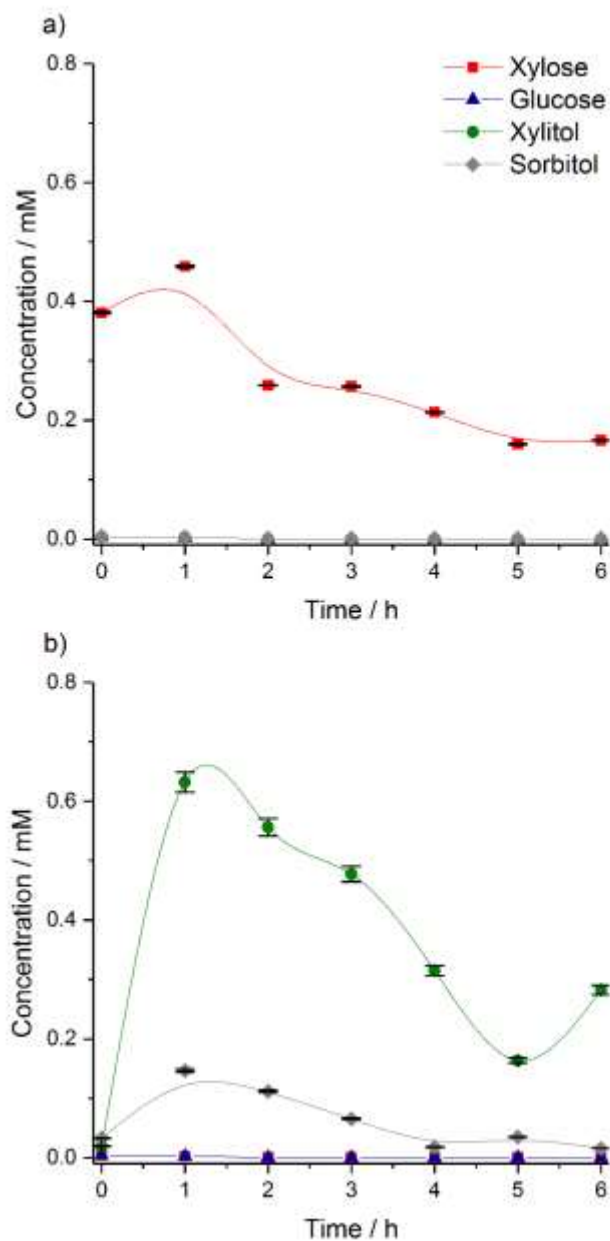


**Figure 3.** Monitoring of the levels of sugars and sugar alcohols in (a) Organosolv liquor and (b) CUB liquor. Experimental conditions: 1) CUB: Poplar wood (17 g), wet Raney Ni (10 g), 2-propanol-water solution (7:3 v/v, 140 mL, as lignin-extracting liquor and H-donor), 200 °C; 2) Organosolv process: the experiment was carried out in the absence of Raney Ni under identical conditions to the CUB. Note that time measurement began upon the liquor reaching a temperature of 200 °C (ca. 60 min ramp time).

Figure 3a reveals that xylose is present in the Organosolv liquor. Notably, however, hexoses were not detected in the Organosolv liquor. As expected, no sugars, but sugar alcohols were detected in the CUB liquor. Interestingly, C<sub>5</sub> and C<sub>6</sub> sugar alcohols were present in the CUB liquor (Figure 3b), with the concentration of xylitol around three times higher than those of xylose in the Organosolv liquor. These findings demonstrate that a significant fraction of the hemicellulose sugars underwent degradation in the Organosolv liquor. Nonetheless, throughout the CUB process, sugar alcohol concentration slowly decreased. This observation suggests that Raney Ni may be utilizing part of the sugar alcohols as H-donors at temperatures of 200 °C. Furthermore, part of the sugar alcohols is known to undergo hydrogenolysis producing lower polyols, as previously reported by us.<sup>1</sup>

The observation that the hydrogenation of hemicellulose sugars prevents the formation of furfurals suggests that, although formic acid can be decomposed by Raney Ni (as outlined in the following sections), the low levels of formic acid in the CUB liquor are more likely to be associated with formation of sugar alcohols, effectively preventing the formation of formic acid *via* the suppression of sequential dehydration of the hemicellulose sugars to furfurals.

To further investigate the reactivity of formic acid and acetic acid in the presence of Raney Ni, 0.2 M solutions of each carboxylic acid in 2-PrOH/H<sub>2</sub>O (7:3 v/v) were subjected to Raney Ni under identical CUB conditions (Figure 4). As previously, formic acid and acetic acid concentration were monitored by LC-MS operating in SIM mode.

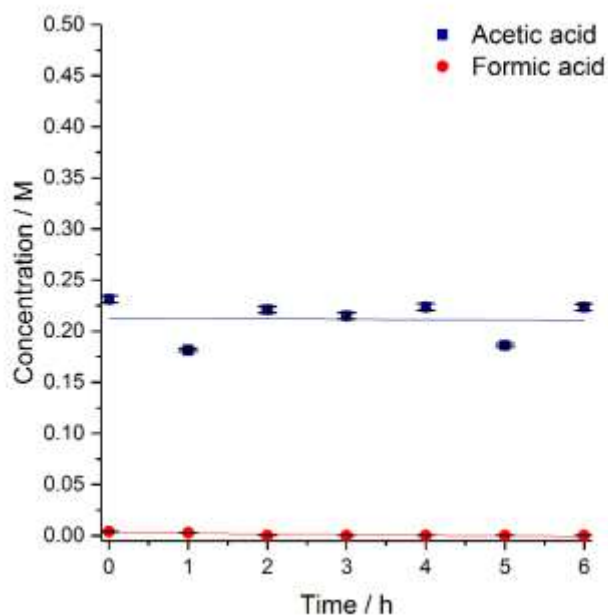


**Figure 4.** Monitoring acetic acid and formic acid concentrations in model experiments under CUB conditions (in the absence of lignocellulose). Experimental conditions: formic acid (0.2 M) or acetic acid (0.2 M) solution in 2-propanol-water (7:3 v/v, 140 mL), Raney Ni (10 g, wet), 200 °C. Note that time measurement began upon the liquor reaching a temperature of 200 °C (ca. 60 min ramp time).

Figure 4 shows that acetic acid levels remain unchanged from the initial 0.2 M concentration throughout the experiment at 200° C, demonstrating that acetic acid is not decomposed *via* H-transfer reactions. Contrastingly, formic acid was fully decomposed already in the temperature ramping stage. This decomposition was associated with an increase in the pressure inside the reactor by about 7 bar (room temperature), indicating that formic acid was transformed into gaseous products (CO<sub>2</sub> and CH<sub>4</sub> as identified by FTIR of the gaseous phase). Conversely, no increase in pressure was noticed for the acetic acid experiment.

### *Impact of formic acid and acetic acid on Raney Ni's hydrogenation activity*

In the previous sections, a complex network of processes associated with the release of acetic acid and formic acid into Organosolv and CUB liquors was discussed. Naturally, these findings give rise to the question of whether these carboxylic acids will affect the performance of Raney Ni for reductive processes during CUB processes. To assess the impact of the exposure of Raney Ni catalyst to acetic acid and formic acid in CUB processes, H-transfer hydrogenation of phenol, employing 2-PrOH as both a solvent and an H-donor, was chosen as a model reaction. By using a pulse injection to give a 0.2 M acetic acid or formic acid solution in a continuous stirred tank reactor (CSTR) operating at 140 °C, the influence of the carboxylic acid upon the catalyst productivity of cyclohexanol (primary product) and cyclohexanone (secondary product) was examined. The acid concentration of 0.2 M corresponds to an extreme condition, as it is much higher than those typically found for formic acid (max. 19 mM, Figure 1) and acetic acid (max. 8 mM, Figure 1). Figure 5 presents the results of the transfer-hydrogenation of phenol performed in a CSTR at 140 °C, revealing the effect of a pulse injection of acetic acid or formic acid.

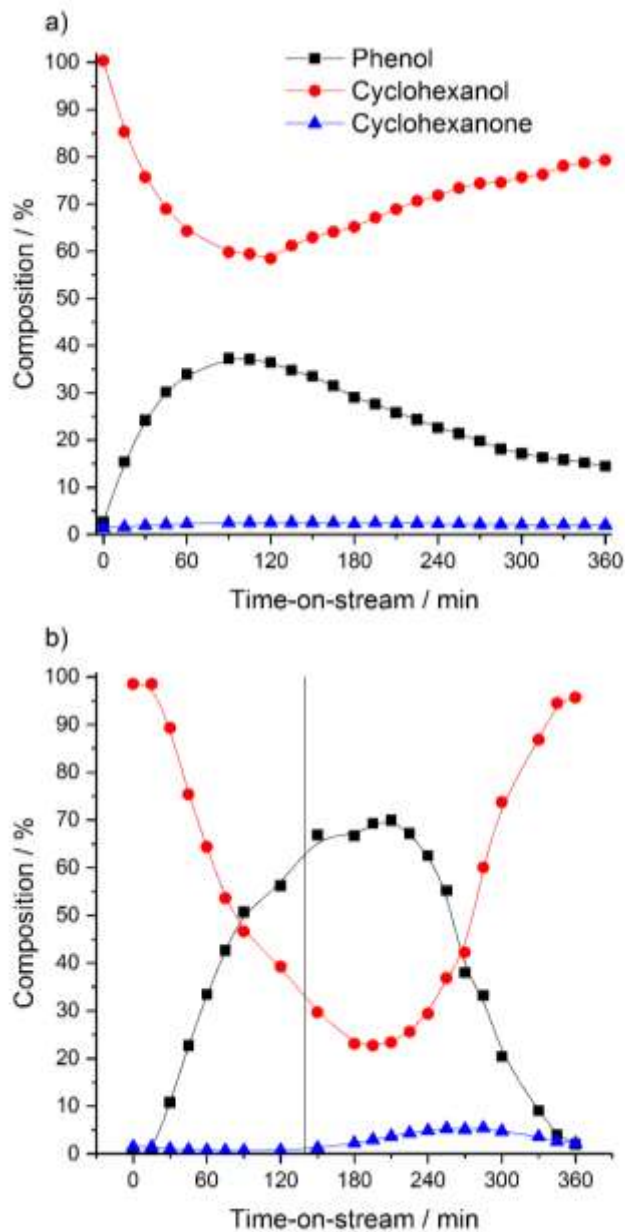
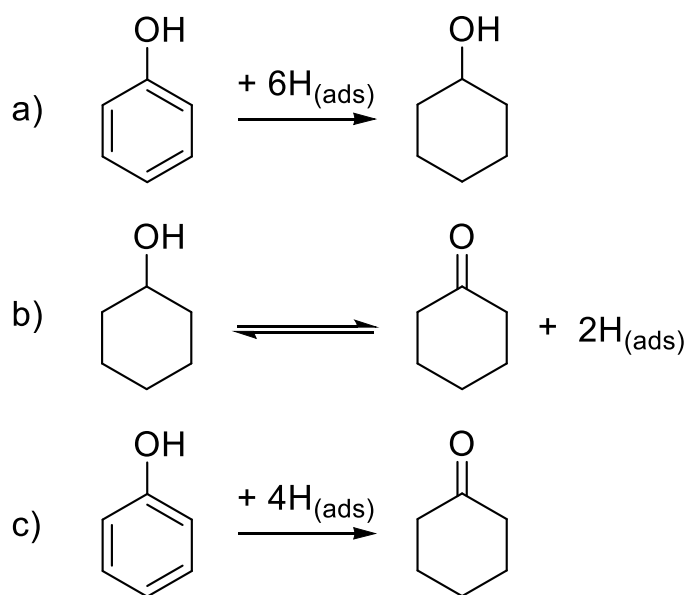


**Figure 5.** Effect of acetic acid or formic acid upon the transfer-hydrogenation of phenol employing 2-PrOH as both solvent and H-donor. At time zero an inhibitor molecule solution was added to the reactor *via* pulse injection, resulting in a concentration of 0.2 M for (a) acetic acid or (b) formic acid in the CSTR operating at 140 °C. The black line in (b) is the point at which the cyclohexanone production increases and the catalyst begins to recover productivity. Experimental conditions: phenol solution in 2-PrOH (0.39 M) at a flow rate of 0.45 mL min<sup>-1</sup>, dry Raney Ni (1.0 g), back pressure 25 bar, 1700 rpm stirring, 140 °C. CSTR volume was 46.5 mL, resulting in a residence time of *ca.* 103 min. For clarity, deviation bars are not presented. The standard deviation was 5% or lower.

Figure 5 shows that the pulse of both acetic acid and formic acid decreased the productivity of cyclohexanol. However, the catalyst partially (in the case of acetic acid) or entirely (in the case of formic acid) recovered its productivity over 6 h time-on-stream. This observation is particularly interesting in the case of formic acid, as the inhibition seems to be reversible, despite the greater initial detrimental impact of formic acid on the catalyst productivity, compared to the effect of acetic acid.



**Scheme 3.** Formation of cyclohexanone from cyclohexanol (a) on a catalyst surface resulting in two adsorbed atoms of hydrogen (b), or direct formation from phenol (c).

The primary product of Raney Ni-catalyzed hydrogen transfer from 2-PrOH to phenol is cyclohexanol (Scheme 3a).<sup>(28)</sup> However, the secondary product, cyclohexanone, also potentially offers essential information regarding the H-transfer processes on the surface of the catalyst, which may change as a consequence of the presence of inhibiting compounds. Cyclohexanone can form in one of two ways, either through the transfer dehydrogenation of

cyclohexanol (Scheme 3b) or as a result of partial hydrogenation of phenol owing to lack of available hydrogen on the catalyst surface (Scheme 3c).

Before the pulse injection of acetic acid or formic acid, cyclohexanone production was found to be *ca.* 2% of the product distribution. After the pulse injection of acetic acid, cyclohexanone production doubled to 4% (Figure 5a). Cyclohexanone production also increased temporarily in the experiment performed with a pulse injection of formic acid (Figure 5b). Notably, the increase in cyclohexanone production occurred in the catalyst reactivation stage, as indicated by the black line in Figure 5b which corresponded roughly to 1.3-times the residence time of the reactor. In the regeneration stage, cyclohexanone production reached 7% of the product distribution or 11% selectivity (*vs.* 2% under standard reaction conditions with no added carboxylic acid).

To further investigate whether the reactivation of the surface of Raney Ni requires hydrogen, the quantity of acetone formed was compared to that of cyclohexanol. Considering the reaction stoichiometry, three moles of acetone should be produced for every mole of cyclohexanol. Figure 6 compares the acetone-to-cyclohexanol molar ratio found in the inhibition experiments.

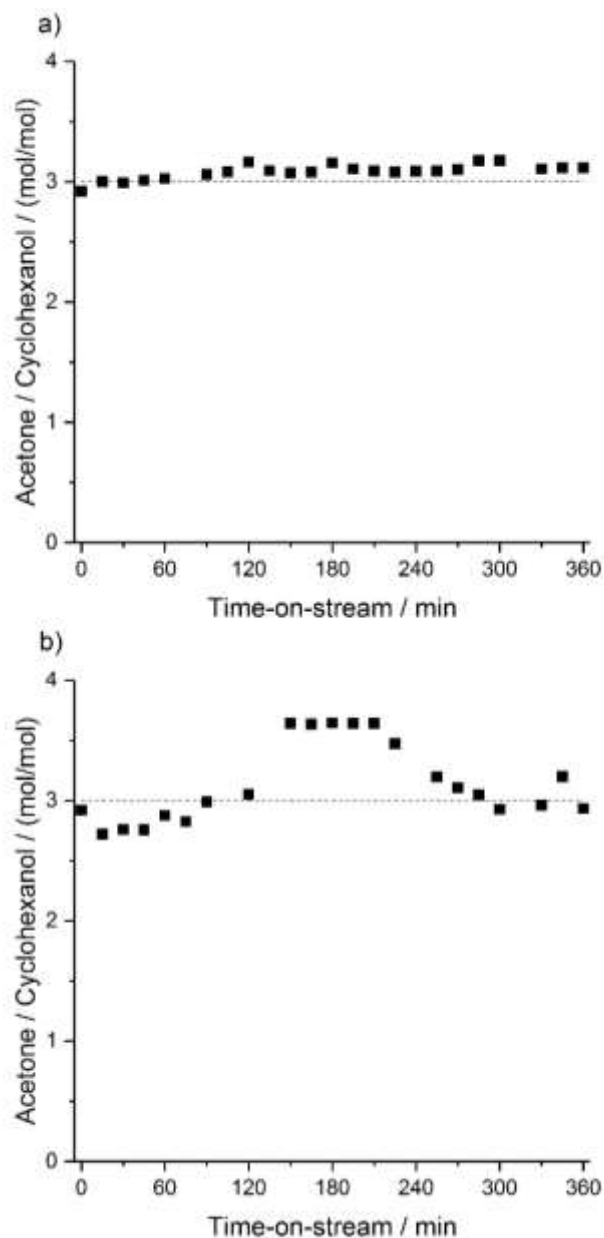


**Figure 6.** Acetone-to-cyclohexanol molar ratio found in transfer-hydrogenation of phenol. At time zero an inhibitor molecule solution was added to the reactor *via* pulse injection, resulting in a concentration of 0.2 M for (a) acetic acid or (b) formic acid in the CSTR at 140 °C. The dotted line represents the acetone-to-cyclohexanol molar ratio expected from the stoichiometry of transfer-hydrogenation of phenol to cyclohexanol. Experimental conditions: a 0.39 M phenol solution in 2-PrOH at a flow rate of 0.45 mL min<sup>-1</sup>, dry Raney Ni (1.0 g), back pressure 25 bar, 1700 rpm stirring, 140 °C. CSTR volume was 46.5 mL, resulting in a residence time of ca. 103 min. For clarity, deviation bars are not presented. The standard deviation was 5% or lower.

Figure 6a shows that the acetone-to-cyclohexanol molar ratio was maintained at *ca.*  $3.0 \pm 0.1$  mol/mol after the pulse injection of acetic acid, in good agreement with the stoichiometric acetone-to-cyclohexanol molar ratio. Moreover, the acetone production is consistent with the acetic acid playing an inhibitory role through a competitive binding interaction with 2-PrOH and/or phenol. Conversely, Figure 6b shows the distinguishing features in the acetone-to-cyclohexanol molar ratio throughout the experiment with formic acid. Indeed, the pulse injection of formic acid initially resulted in decreased acetone production, suggesting that either part of the H-content stored in Raney Ni is utilized for the hydrogenation process due to surface poisoning by formic acid, or that formic acid could be utilized as an H-donor. In contrast, between 120 and 240 min of time-on-stream, the acetone-to-cyclohexanol molar ratio reached a value of 3.6, indicating that part of 2-PrOH was utilized in the regeneration of Raney Ni's performance.

To address the inhibiting effects of acetic acid and formic acid on Raney Ni, and identify the species formed as a result of the adsorption of acetic acid or formic acid, the liquid-solid interface of Raney Ni was analyzed by ATR-IR spectroscopy. This technique has previously been employed in the characterization of organic adsorbates at the liquid-solid interface of Raney Ni.<sup>(29),(34),(35)</sup> To obtain the ATR-IR spectra, Raney Ni was contacted with a 1  $\mu$ M formic acid or acetic acid in cyclohexane. Figure 7 compares the ATR-IR spectra of the acid solution and acid adsorbed on Raney Ni.

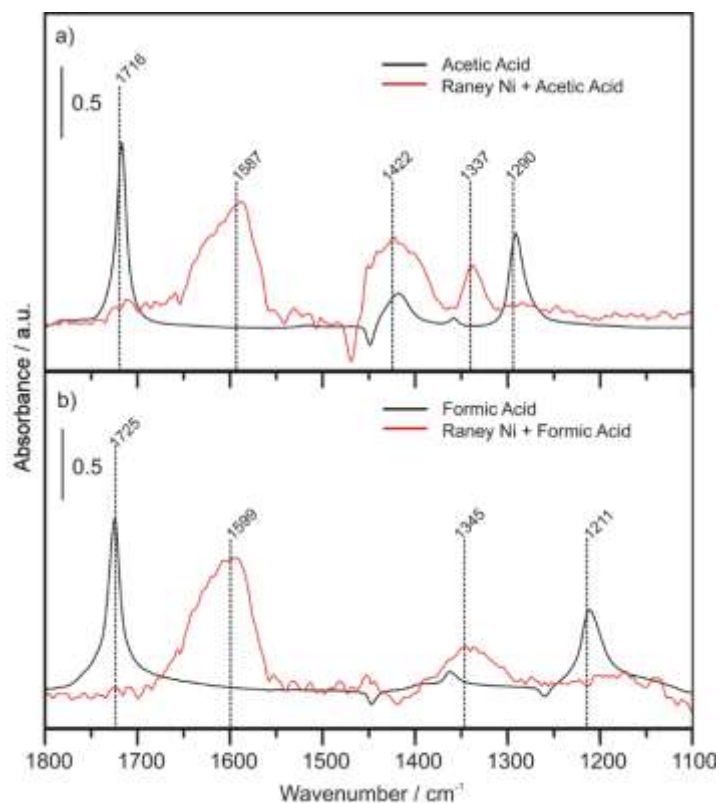


**Figure 7.** ATR-IR spectra of adsorbed carboxylic acids on Raney Ni: a) acetic acid, and b) formic acid. Black traces show the spectra of 1 mM acidic solutions in cyclohexane, while red traces are ATR-IR spectra of Raney Ni exposed to 1  $\mu$ M acid solutions in cyclohexane. A low concentration was employed to collect the ATR-IR spectra with no contribution of non-adsorbed acidic species in the liquid phase.

In the ATR-IR spectra of the liquid-solid interface of Raney Ni, the signals for  $\nu(\text{CO})$  (acetic acid: 1725  $\text{cm}^{-1}$ ; formic acid: 1716  $\text{cm}^{-1}$ ) and the  $\nu(\text{C-OH})$  (acetic acid: 1290  $\text{cm}^{-1}$ ; formic acid: 1211  $\text{cm}^{-1}$ ), related to the carboxylic acid dimers in solution, were replaced with two new bands assigned to  $\nu_{\text{sym}}(\text{OCO})$  and  $\nu_{\text{asym}}(\text{OCO})$ .<sup>(36),(37),(38)</sup> These IR bands suggest that the carboxylic acid dimers in solution are converted into carboxylate species on Raney Ni surface. Carboxylates can coordinate to metals in several ways, for example as a unidentate ligand, a bidentate/chelating ligand, a bridging bidentate ligand or as a monoatomic bridging ligand.<sup>(39)</sup> Each orientation on the surface will have its own stability, which could be related

to the effects of acetic acid and formic acid on the transfer-hydrogenation of phenol, as shown in Figures 5 and 6. Notably, from the IR data, it is possible to infer the coordination of carboxylates on a surface. Typically, a coordination differing from a symmetrical bidentate/chelating ligand will break the equivalent carbon-oxygen bond order of  $\text{RCOO}^-$  bidentate ligand (i.e. both carbon-oxygen bonds with a bond order of  $1^{1/2}$ ), generating inequivalent carbon-oxygen bond orders (i.e., for a unidentate coordination, one carbon-oxygen bond with a bond order of 1 and the other of 2, as in an ester group). Such a change in carbon-oxygen bond orders directly translates into substantial shifts in both  $\nu_{\text{sym}}(\text{OCO})$  and  $\nu_{\text{asym}}(\text{OCO})$ . In this manner, the separation  $\Delta\nu$  ( $[\nu_{\text{asym}}(\text{OCO})-\nu_{\text{sym}}(\text{OCO})]$ ) serves as an indicator of the nature of the carboxylate coordination.<sup>(39)</sup>

From the ATR-IR data, Raney Ni exposed to acetic acid exhibits  $\nu_{\text{sym}}(\text{OCO})$  and  $\nu_{\text{asym}}(\text{OCO})$  for acetate at around 1422 and 1587  $\text{cm}^{-1}$ , respectively, leading to a  $\Delta\nu$  value of 165  $\text{cm}^{-1}$  (Figure 7a). Such a  $\Delta\nu$  compares to that found for anhydrous sodium acetate [ $\nu_{\text{sym}}(\text{OCO})$ : 1414  $\text{cm}^{-1}$ ;  $\nu_{\text{asym}}(\text{OCO})$ : 1578  $\text{cm}^{-1}$ ;  $\Delta\nu$ : 164  $\text{cm}^{-1}$ ] in which the acetate ion presents equivalent carbon-oxygen bond orders. Hence, the spectral data indicates bidentate coordination of acetate ions to Raney Ni surface. In turn, formate species adsorbed on the catalyst surface displayed  $\nu_{\text{sym}}(\text{OCO})$  and  $\nu_{\text{asym}}(\text{OCO})$  at around 1599 and 1345  $\text{cm}^{-1}$ , respectively, giving a  $\Delta\nu$  value of 254  $\text{cm}^{-1}$  (Figure 7b). These values are considerably similar to the ionic counterpart, sodium formate [ $\nu_{\text{sym}}(\text{OCO})$ : 1363  $\text{cm}^{-1}$ ;  $\nu_{\text{asym}}(\text{OCO})$ : 1604  $\text{cm}^{-1}$ ;  $\Delta\nu$ : 241  $\text{cm}^{-1}$ ], again indicating a bidentate coordination to Raney Ni surface.

Considering that both acetate and formate show bidentate coordination to Raney Ni surface, the distinguished effects of these acids on the performance of phenol's transfer-hydrogenation are apparently not associated with the adsorption of such anions. Incidentally,

as nickel is a base metal, it is expected that Raney Ni can oxidize in the presence of an acid. To examine whether extensive oxidation of the catalyst takes place, Ni K-edge XANES analysis was performed. Figure 8 presents the normalized Ni K-edge XANES spectra of freshly-prepared Raney Ni and catalyst samples suspended in a 0.1 mM solution of acetic acid or formic acid in 7:3 (v/v) 2-PrOH/H<sub>2</sub>O. For comparison, the normalized Ni K-edge XANES spectra of a Ni(0) foil and Ni(HCOO)<sub>2</sub> are also shown in Figure 8.

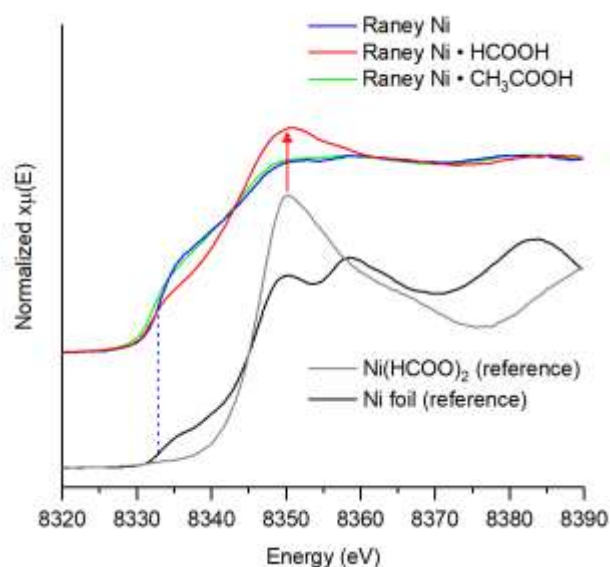


**Figure 8.** Ni K-edge XANES spectra of freshly-prepared Raney Ni and catalyst samples suspended in a 0.1 mM solution of acetic acid or formic acid in 7:3 (v/v) 2-PrOH/H<sub>2</sub>O. For comparison, Ni K-edge XANES spectra of a Ni(0) foil and Ni(HCOO)<sub>2</sub>, as reference materials, are also presented.

XANES spectrum of the freshly-prepared Raney Ni indicates that the chemical environment around the Ni atoms are identical to the Ni foil (reference). The threshold-onset feature of the freshly-prepared Raney Ni at the Ni K edge (8333 eV) indicates that the initial catalyst is not oxidized.<sup>(40),(41)</sup> Notably, the XANES spectrum of Raney Ni exposed to acetic acid showed a shift by -2 eV in the threshold-onset feature, probably caused by a charge-

transfer from acetate to nickel, owing to acetate chemisorption. Importantly, the absence of Ni(II) characteristic single white line at ~8350 eV demonstrates that Raney Ni was not extensively oxidized by acetic acid. By stark contrast, in the XANES spectrum of Raney Ni exposed to formic acid, the first spectrum feature at 8333 eV decreased in intensity. In addition, the appearance of the single white line at 8350 eV, similar to that found in the XANES spectrum of Ni(HCOO)<sub>2</sub>, demonstrated that the oxidation of Raney Ni by formic acid was more profound and not only restricted to the uppermost surface layer. To conclude, XANES results indicate that the Raney Ni oxidation extends considerably deep into the bulk.

Therefore, revisiting the results presented in Figure 6, it becomes clear that, in the regeneration phase of Raney Ni, the high acetone-to-cyclohexanol molar ratio of 3.6 is associated with catalyst reduction. Nonetheless, other processes may also be consuming 2-PrOH as the H-donor. Indeed, in the experiment of transfer-hydrogenation of phenol in the presence of formic acid, together with CO<sub>2</sub>, a typical product of decomposition of formic acid when serving as an H-donor,<sup>(42)-(45)</sup> we also detected methane in the gas-phase. This finding suggests the formation of methane may take place as an H-transfer reaction sequential to the formation of CO<sub>2</sub>, thus consuming additional 2-PrOH. Work is in progress in our group to assess the formation of methane in the conversion of formic acid in the presence of Raney Ni under H-transfer conditions.

#### *Effect of temperature on Raney Ni inhibition*

To assess the effect of temperature on the Raney Ni inhibition by acetic acid or formic acid, the pulse injection experiments of H-transfer hydrogenation of phenol were carried out at various temperatures. The residence time of the compounds in the reactor was unaffected

by the increase in the temperature, due to the constant flow rate and constant backpressure (25 bar). We defined the *inhibition strength* as the maximum concentration of phenol measured during the reaction (due to suppression of transfer hydrogenation of phenol to cyclohexanol). Figure 9 presents the inhibition strength as a function of the temperature.

For both formic acid and acetic acid, an increase in the reaction temperature was beneficial to decrease catalyst inhibition. However, temperature effects appear much more significant for formic acid, resulting in a complete absence of an inhibitory effect at the highest temperatures. This observation is most likely related to the decomposition of formate surface species. Indeed, anhydrous nickel formate decomposes at temperatures around 200°C, forming Ni, CO/CO<sub>2</sub> and H<sub>2</sub>O.<sup>(46)-(48)</sup> In the case of acetic acid, inhibition is not fully overcome by increasing process temperatures. In this manner, acetic acid still exerts a small detrimental effect in the H-transfer reductive processes catalyzed by Raney Ni.

Extrapolating the trends found in Figure 9 to a temperature of 180°C, currently, the minimum temperature required for extensive lignin extraction and, therefore, for the lignin-first deconstruction of lignocellulose, shows that formic acid will not inhibit Raney Ni. Importantly, owing to the hydrogenation of sugars to sugar alcohols, thus mitigating the formation of formic acid, the levels of formic acid found in the CUB process are dramatically reduced. Therefore, although interesting from the perspective of understanding the fate of formic acid in the presence of Raney Ni, formic acid is unlikely to pose any problem to Raney Ni performance in the CUB process. In the case of acetic acid, there will be a slight reduction in the performance of Raney Ni. Nonetheless, the acetic acid effect on the hydrogenation activity of Raney Ni is notoriously small at temperatures higher than 180 °C at which lignin-first biorefining processes are often performed.

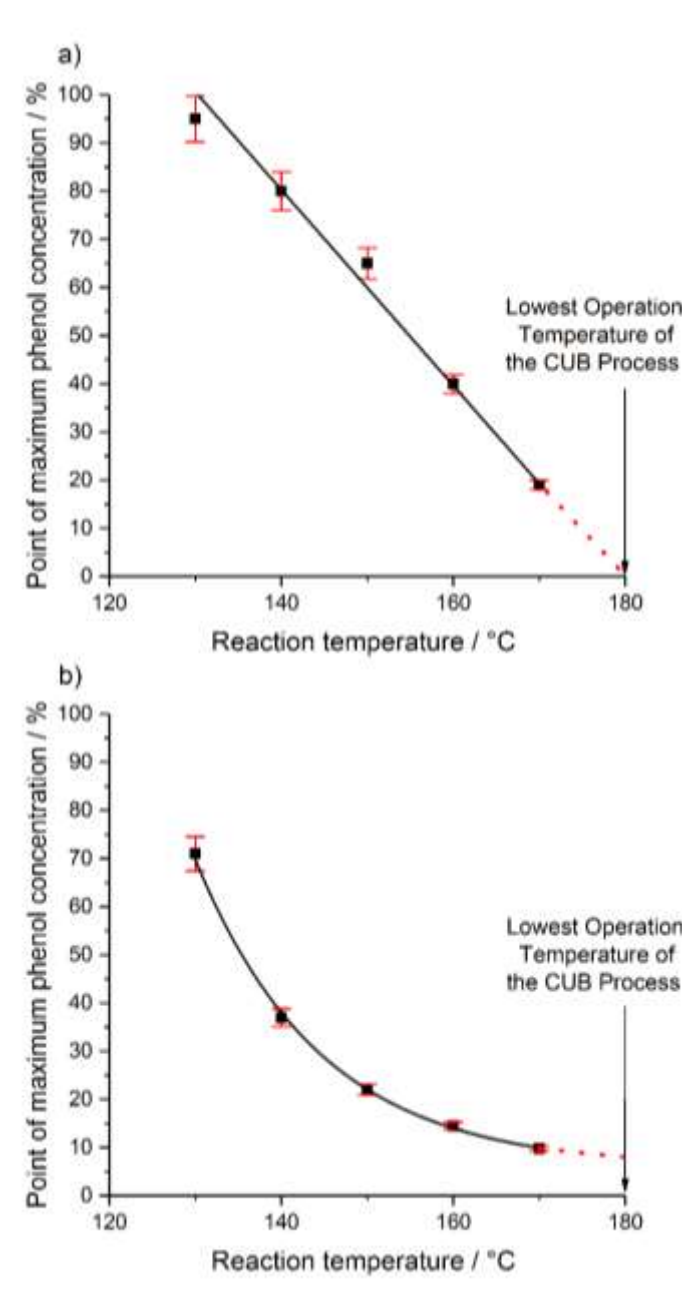


**Figure 9.** Dependence of inhibition strength of (a) formic acid and (b) acetic acid, as defined by the point of maximum phenol concentration in the stream. Experimental conditions: phenol solution in 2-PrOH (0.39 M) at a flow rate of  $0.45 \text{ mL min}^{-1}$ , dry Raney Ni (1.0 g), pulse injection of the inhibitor molecule solution to result in an initial solution concentration of 0.2 M formic acid or 0.2 M acetic acid in 2-PrOH with 1700 rpm stirring and backpressure 25 bar at the indicated temperatures.

## Conclusions

We have demonstrated that Raney Ni catalyst impacts on the formation and fate of acetic acid and formic acid in the lignin-first biorefining. The influence of Raney Ni on the carboxylic acid formation is especially crucial in the case of formic acid, as its content in CUB liquors was found to be significantly lower than for Organosolv processes. The low levels of formic acid were attributed to the preferential hydrogenation of sugars into sugar alcohols in the presence of the Raney Ni, preventing sugar degradation, and ultimately the formation of formic acid. The ability of Raney Ni to decompose formic acid by H-transfer reactions becomes thus redundant. Conversely, Raney Ni did not appear to promote acetic acid decomposition through H-transfer reactions, rather the concentration of acetic acid remained stable during CUB being mainly governed by the impact of the overall acid content on the deacetylation equilibrium. However, continuous exposure of Raney Ni to these carboxylic acids may impact its performance, as it was observed by pulse injection experiments that both acetic acid and formic acid have a detrimental impact on Raney Ni catalytic performance in a model H-transfer hydrogenation of phenol, with the most potent inhibition observed for formic acid. Nonetheless, unlike acetic acid, the performance of Raney Ni is wholly recovered over time-on-stream for formic acid. Both carboxylic acids were observed by ATR-IR spectroscopy to interact with the surface of Raney Ni as acetate and formate in bidentate coordination, though competing with 2-PrOH and phenol for the active sites on the catalyst surface. Additionally, in the case of formic acid, Raney Ni oxidation followed by a reactivation of the catalyst took place, increasing the quantity of 2-PrOH consumed by the lignin-first process. Our data also suggest that 2-PrOH could also be involved in other H-

transfer processes, namely the conversion of CO<sub>2</sub> (from the decomposition of formic acid) into methane.

Even though the impact of formic acid and acetic acid on Raney Ni performance is more significant at low temperatures, inhibition seems to be entirely (for formic acid) or significantly (for acetic acid) overcome by increases in process temperature. This observation indicates that, under the conditions of lignin-first deconstruction of lignocellulose, formic acid is unlikely to inhibit Raney Ni performance, whereas acetic acid might only be detrimental upon long exposure times.

## **Experimental**

### *Organosolv and CUB of poplar wood*

Poplar wood (17 g) and a mixture of 2-propanol and water (7:3 v/v, 140 mL) were placed in a 250 mL autoclave and heated up to the desired temperature (200 °C). For the CUB process, Raney Ni (10 g, wet) was also added to the reaction mixture. The reaction proceeded under autogenous pressure for a total of 6 h, and aliquots of the reaction mixture were taken at defined times and set aside for LC-MS analysis.

### *Model experiments with cellulose acetate*

Cellulose acetate (0.25 g, average Mn ~50,000 g mol<sup>-1</sup> by GPC) was added to a mixture of 2-propanol and water (7:3 v/v, 140 mL) and placed in a 250 mL autoclave, which was heated up to 200 °C. The reaction proceeded under autogenous pressure for a total of 6 h, and several aliquots of the reaction mixture were taken at different times. In a second experiment, 15 mM

was added to the reaction mixture. In order to analyze the content of acetic acid and formic acid, samples were centrifuged, filtered and analyzed by LC-MS.

#### *Reactivity of formic acid and acetic acid*

Formic acid or acetic acid (0.2 M) and a mixture of 2-propanol and water (7:3 v/v, 140 mL) were placed in a 250 mL autoclave and heated up to the desired temperature (200 °C). Raney Ni (10 g, wet) was also added to the reaction mixture. The reaction proceeded under autogenous pressure for a total of 6 h, and several aliquots of the reaction mixture were collected at different times. For determination of formic acid and acetic acid concentrations, samples were diluted in water, centrifuged and filtered before being analyzed by LC-MS.

#### *LC-MS analysis*

Liquor samples were then diluted (1:1) in Milli-Q water, centrifuged and filtered before being analyzed in a Shimadzu LC-MS 2020 system using an electrospray ionization (ESI) MS ion source and operating in Selected Ion Monitoring (SIM) mode for the detection of formic acid, acetic acid, C<sub>5</sub>/C<sub>6</sub> sugars and sugars alcohols. The system was equipped with a TSKgel Amide-80 3.0×100 mm column operating at 70 °C. The mobile phase was a mixture of acetonitrile and water (ACN/H<sub>2</sub>O: 75:25 v/v) at a flow rate of 0.35 mL min<sup>-1</sup>. A gradient method for the mobile phase was applied. Within the initial 5 min, the mobile phase was maintained at an ACN/H<sub>2</sub>O concentration of 75:25 (v/v); between 5-10 min, it was linearly decreased to 40:60 (v/v) ACN/H<sub>2</sub>O. Finally, mobile phase ACN/H<sub>2</sub>O concentration was increased to 75:25 (v/v) from 10-14 min, remaining at this concentration until the end of the

run (15 min). To allow for high sensitivity for quantification of the sugars and sugar alcohols, a post-column addition of a solution of methanol and chloroform (4:1 v/v, 0.075 mL min<sup>-1</sup>) was made. This procedure allows for the formation of the corresponding [carbohydrate-Cl]<sup>-</sup> ions, dramatically increasing the sensitivity for sugars and sugars alcohols.

### *Inhibition experiments*

Catalyst inhibition experiments were performed in a continuous stirred tank reactor (CSTR) fed with a 0.39 M phenol solution in 2-PrOH by a HPLC pump. Under argon atmosphere, dry Raney Ni (1.0 g) suspended in 2-PrOH was transferred into a 46.5-mL reactor. Next, to shorten the initial equilibration time, Raney Ni was held in the reactor with a magnet as the 2-PrOH was removed from the reactor and replaced with the 2-PrOH-phenol solution. The reactor was sealed, flushed with Ar and connected into the reactor set-up. A flow rate of 0.45 mL min<sup>-1</sup> of the 2-PrOH-phenol solution was initiated, generating a backpressure of ca. 25 bar. The reactor was heated to 120 °C at which point stirring (1700 rpm) was initiated. The system was then heated up to the reaction temperature. The reaction continued until a steady state conversion of ca. 100% was achieved at which point an inhibitor molecule solution (1 mL) was added to the reactor *via* the Rheodyne 7010 Sample Injector to result in an initial inhibitor molecule concentration of 0.2 M. The concentration of phenol was analyzed by in-line ultraviolet-visible spectroscopy (UV-Vis) (Agilent 8453 UV-Visible spectrophotometer) equipped with a continuous flow cell (Hellma Analytics Quartz SUPRASIL<sup>®</sup> 0.1-mm pathlength flow cell). The wavelength was selected outside the maximum absorbance for phenol (286 nm) to have an extended linear range of absorption at high concentration of phenol.

The formation of cyclohexanol and cyclohexanone in the inhibition experiments was monitored using gas chromatography (GC) analysis. Samples were collected from continuous flow experiments using a Gerstel Multi-Purpose-Sampler. All samples were analyzed on a GC 6850 Agilent equipped with an HP-INNOWax column (30 m, 0.25 mm internal diameter,  $d_f$  0.25  $\mu\text{m}$ ) with an injection temperature of 280 °C and a 10:1 split ratio of H<sub>2</sub> carrier gas. The temperature program was as follows; an initial isothermal step at 35 °C for 2 min, temperature then increased from 35 to 120 °C (ramp rate of 100 °C min<sup>-1</sup>), followed by an increase to 200 °C at the same ramp rate. Finally, the temperature program was finished with an isothermal step at 200 °C for 5 min.

#### *ATR-IR spectroscopy measurements*

The instrument used for the *in situ* monitoring of surface adsorption using ATR-FTIR is described in detail elsewhere. A film of Raney Ni was deposited on the surface of the ZnSe crystal in a custom built mini-glove-box, as described previously.<sup>(49)</sup> The film was then sealed into the ATR cell under Ar atmosphere and transferred to the continuous flow set-up.<sup>(49)</sup> Argon was removed from the cell with a cyclohexane solution at a flow rate of 0.5 mL min<sup>-1</sup>, after which the flow rate was increased to 2.7 mL min<sup>-1</sup>. A background spectrum was collected under a convective flow of cyclohexane at a flow rate of 2.7 mL min<sup>-1</sup>. The film was then treated with a solution containing 1  $\mu\text{mol}$  of formic acid and acetic acid and 5  $\mu\text{mol}$  for propionic in cyclohexane, with an ATR-IR spectrum collected every 20 s.

### *Ni K-edge XANES*

For measurement, the wet Raney Ni samples were dispersed homogeneously in petroleum jelly. XANES analyses were performed using the transmission mode at beamline “DXAS” of the Brazilian Synchrotron Light Laboratory (LNLS) which was operating at 1.37 GeV, at the Ni K-edge (8333 eV).<sup>(50)</sup> To monochromatize the incoming radiation, a curved Si(111) monochromator, operating in Bragg mode in an X-ray range from 4 keV up to 14 keV and focusing it on the sample, was used. For the detection, a CCD solid-state detector was employed. Energy calibration and normalization of the spectra were performed using the ATHENA software. The catalyst spectra were compared against reference spectra of Ni(OH)<sub>2</sub> (Ni<sup>+2</sup>) and nickel foil (Ni<sup>0</sup>) collected under the same conditions as those for the samples.

### **Acknowledgements**

This work was also conducted with the financial support provided by the ERC Consolidator Grant LIGNINFIRST (Project Number: 725762). The authors are thankful to Brazilian Synchrotron Light Laboratory (LNLS) for measurements in the DXAS beamline (Project Number: 20160732). RR and MK are grateful to Dr Fabian Meemken (ETH Zürich) for granting us the access to the ATR-IR facilities.

### **References**

- (1) Ferrini, P.; Rinaldi, R. Catalytic biorefining of plant biomass to non-pyrolytic lignin bio-oil and carbohydrates through hydrogen transfer reactions. *Angew. Chem. Int. Ed.* **2014**, *53*, 8634–8639.

- (2) Rinaldi, R.; Jastrzebski, R.; Clough, M. T.; Ralph, J.; Kennema, M; Bruijninx, P. C. A.; Weckhuysen, B. M. Paving the way for lignin valorisation: Recent advances in bioengineering, biorefining and catalysis, *Angew. Chem. Int. Ed.* **2016**, *55*, 8164–8215.
- (3) Rinaldi R. Plant biomass fractionation meets catalysis. *Angew. Chem. Int. Ed.* **2014**, *53*, 8559–8560.
- (4) Renders, T.; Van den Bosch, S.; Koelewijn; S.-F.; Schutyser, W.; Sels, B. F. Lignin-first biomass fractionation: the advent of active stabilization strategies. *Energy Environ. Sci.* **2017**, *10*, 1551–1557.
- (5) Schutyser, W.; Renders, T.; Van den Bosch, S.; Koelewijn, S.-F.; Beckham, G. T.; Sels, B. F. Chemicals from lignin: an interplay of lignocellulose fractionation, depolymerization, and upgrading. *Chem. Soc. Rev.* **2018**, *47*, 852–908.
- (6) Rinaldi, R. in G. T. Beckham (Ed.), *Lignin Valorization: Emerging Approaches*, Chapter 5: Early-stage conversion of lignin over hydrogenation catalysts, Royal Society of Chemistry, UK, **2018**, p. 108–127, DOI 10.1039/9781788010351-00108.
- (7) Chesi, C.; de Castro, I. B. D.; Clough, M. T.; Ferrini, P.; Rinaldi, R. The influence of hemicellulose sugars on product distribution of early-stage conversion of lignin oligomers catalysed by Raney Nickel. *ChemCatChem* **2016**, *8*, 2079–2088.

(8) Other not previously cited examples of lignin-first biorefining are listed here, grouped by catalytic system: **(mechanocatalytic biorefining)** a) Calvaruso, G.; Burak, J.; Clough, M. T.; Kennema, M.; Meemken, F.; Rinaldi, R. On the meaning and origins of lignin recalcitrance: A critical analysis of the catalytic upgrading of lignins obtained from mechanocatalytic biorefining and organosolv pulping. *ChemCatChem* **2017**, *9*, 2627–2700; **(noble-metal/C catalysts)** b) Van den Bosch, S.; Schutyser, W.; Koelewijn, S.-F.; Renders, T.; Courtin, C.; Sels, B. Tuning the lignin oil OH-content with Ru and Pd catalysts during lignin hydrogenolysis on birch wood. *Chem. Comm.* **2015**, *51*, 13158–13161; c) Van den Bosch, S.; Schutyser, W.; Vanholme, R.; Driessen, T.; Koelewijn, S.-F.; Renders, T.; De Meester, B.; Huijgen, W. J. J.; Dehaen, W.; Courtin, C.; Lagrain, B.; Boerjan, W.; Sels, B. F. Reductive lignocellulose fractionation into soluble lignin-derived phenolic monomers and dimers and processable carbohydrate pulps. *Energy Environ. Sci.* **2015**, *8*, 1748–1763; d) Yan, N.; Zhao, C.; Dyson, P. J.; Wang, C.; Liu, L. T.; Kou, Y. Selective degradation of wood lignin over noble-metal catalysts in a two-step process. *ChemSusChem* **2008**, *1*, 626–629; e) Klein, I.; Marcum, C.; Kenttämä, H.; Abu-Omar, M. M. Mechanistic investigation of the Zn/Pd/C catalyzed cleavage and hydrodeoxygenation of lignin. *Green Chem.* **2016**, *18*, 2399–2405; f) Parsell, T.; Yohe, S.; Degenstein, J.; Jarrell, T.; Klein, I.; Gencer, E.; Hewetson, B.; Hurt, M.; Kim, J. I.; Choudhari, H.; Saha, B.; Meilan, R.; Mosier, N.; Ribeiro, F.; Delgass, W. N.; Chapple, C.; Kenttämä, H. I.; Agrawal, R.; Abu-Omar, M. M. A synergistic biorefinery based on catalytic conversion of lignin prior to cellulose starting from lignocellulosic biomass. *Green Chem.* **2015**, *17*, 1492–1499; g) Kumaniaev, I.; Subbotina, E.; Sävmarker, J.; Larhed, M.; Galkin, M. V.; Samec, J. S. M. Lignin depolymerization to monophenolic

compounds in a flow-through system. *Green Chem.* **2017**, *19*, 5767–5771; h) Galkin, M. V.; Dahlstrand, C.; Samec, J. S. M. Mild and robust redox-neutral Pd/C-catalyzed lignol  $\beta$ -O-4' bond cleavage through a low-energy-barrier pathway. *ChemSusChem* **2015**, *8*, 214–2142; i) Galkin, M. V.; Samec, J. S. M. Selective route to 2-propenyl aryls directly from wood by a tandem organosolv and palladium-catalysed transfer hydrogenolysis. *ChemSusChem* **2014**, *7*, 2154–2158; j) Galkin, M. V.; Sawadjoon, S.; Rohde, V.; Dawange, M.; Samec, J. S. M. Mild heterogeneous palladium-catalyzed cleavage of  $\beta$ -O-4'-ether linkages of lignin model compounds and native lignin in air. *ChemCatChem* **2013**, *6*, 179–184; **(Ni/C catalysts)** l) Luo, H.; Klein, I. M.; Jiang, Y.; Zhu, H. Y.; Liu, B. Y.; Kenttamaa, H. I.; Abu-Omar, M. M. Total utilization of Miscanthus biomass, lignin and carbohydrates using earth abundant nickel catalyst. *ACS Sustainable Chem. Eng.* **2016**, *4*, 2316–2322; k) Klein, I.; Saha, B.; Abu-Omar, M. M. Lignin depolymerization over Ni/C catalyst in methanol, a continuation: effect of substrate and catalyst loading. *Catal. Sci. Technol.* **2015**, *5*, 3242–3245; m) Anderson, E. M.; Katahira, R.; Reed, M.; Stone, M. L.; Hülsey, M. J.; Beckham, G. T.; Román-Leshkov, Y. Kinetic studies of lignin solvolysis and reduction by reductive catalytic fractionation decoupled in flow-through reactors. *ACS Sustainable Chem. Eng.* **2018**, *6*, 7951–7959; n) Resch, M. G.; Karp, E. M.; Beckham, G. T.; Román-Leshkov, Y. Reductive catalytic fractionation of corn stover lignin, *ACS Sustainable Chem. Eng.* **2016**, *4*, 6940–6950; **(acid-catalyzed depolymerization in the presence of protecting agents)** o) Deuss, P. J.; Scott, M.; Tran F.; Westwood, N. J.; de Vries, J. G.; Barta, K. Aromatic monomers by *in situ* conversion of reactive intermediates in the acid-catalyzed depolymerization of lignin. *J. Am. Chem. Soc.* **2015**, *137*, 7456–7467; **(formaldehyde as a protecting group)** p) L. Shuai, M. T. Amiri, Y. M. Questell-

- Santiago, F. Héroguel, Y. Li, H. Kim, R. Meilan, C. Chapple, J. Ralph, J. S. Luterbacher. Formaldehyde stabilization facilitates lignin monomer production during biomass depolymerization. *Science* **2016**, *354*, 329-333.
- (9) Deneyer, A.; Renders, T.; Van Aelst, J.; Van den Bosch, S.; Gabriëls, D.; Sels, B. F. Alkane production from biomass: chemo-, bio- and integrated catalytic approaches. *Curr. Opin. Chem. Biol.* **2015**, *29*, 40–48.
- (10) Galkin, M. V.; Samec, J. S. M. Lignin valorization through catalytic lignocellulose fractionation: A fundamental platform for the future biorefinery. *ChemSusChem* **2016**, *9*, 1544–1558.
- (11) Deuss, P. J.; Barta, K. From models to lignin: Transition metal catalysis for selective bond cleavage reactions. *Coord. Chem. Rev.* **2016**, *306*, 510–532.
- (12) Sun, Z.; Fridrich, B.; de Santi, A.; Elangovan, S.; Barta, K. Bright side of lignin depolymerization: Toward new platform chemicals. *Chem. Rev.* **2018**, *118*, 614–678.
- (13) Ferrini, P.; Rezende, C. A.; Rinaldi, R. Catalytic upstream biorefining through hydrogen transfer reactions: Understanding the process from the pulp perspective *ChemSusChem* **2016**, *9*, 3171–3180.
- (14) Garrote, G.; Dominguez, H.; Parajo, J. C. Interpretation of deacetylation and hemicellulose hydrolysis during hydrothermal treatments on the basis of the severity factor. *Process Biochem.* **2002**, *37*, 1067–1073.
- (15) Garrote, G.; Domínguez, H.; Parajó, J. C. Study on the deacetylation of hemicelluloses during the hydrothermal processing of Eucalyptus wood. *Holz als Roh- und Werkstoff* **2001**, *59*, 53–59.

- (16) Samuel, R.; Foston, M.; Jiang, N.; Allison, L.; Ragauskas, A. J. Structural changes in switchgrass lignin and hemicelluloses during pretreatments by NMR analysis. *Polym. Degrad. Stabil.* **2011**, *96*, 2002–2009.
- (17) Sundqvist, B.; Karlsson, O.; Westermark, U. Determination of formic-acid and acetic acid concentrations formed during hydrothermal treatment of birch wood and its relation to colour, strength and hardness. *Wood Sci. Techn.* **2006**, *40*, 549–561.
- (18) Jönsson, L. J.; Martín, C. Pretreatment of lignocellulose: Formation of inhibitory by-products and strategies for minimizing their effects. *Bioresour. Technol.* **2016**, *199*, 103–112.
- (19) Oregui-Bengoechea, M.; Gandarias, I.; Arias, P. L.; Barth, T. Unraveling the role of formic acid and the type of solvent in the catalytic conversion of lignin: A holistic approach. *ChemSusChem* **2017**, *10*, 754–766.
- (20) Fengel, D.; Wegener, G. *Wood: Chemistry, Ultrastructure, Reactions*, de Gruyter, Berlin, **1983**.
- (21) Gosselink, R. J. A.; van Dam, J. E. G.; Zomers, F. H. A. Combined HPLC analysis of organic acids and furans formed during Organosolv pulping of fiber hemp. *J. Wood Chem. Technol.* **1995**, *15*, 1–25.
- (22) Sannigrahi, P.; Ragauskas, A. J.; Tuskan, G. A. Poplar as a feedstock for biofuels: A review of compositional characteristics. *Biofuels, Bioprod. Bioref.* **2010**, *4*, 209–226.
- (23) Flannelly, T.; Lopes, M.; Kupiainen, L.; Dooley, S.; Leahy, J. J. Non-stoichiometric formation of formic and levulinic acids from the hydrolysis of biomass derived hexose carbohydrates. *RSC Adv.* **2016**, *6*, 5797–5804.

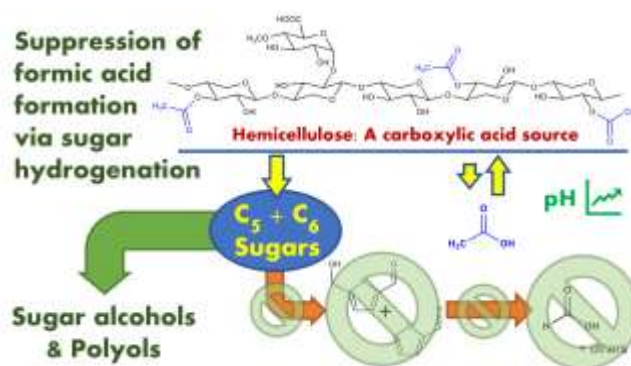
- (24) Qi, L.; Mui, Y. F.; Lo, S. W.; Lui, M. Y.; Akien, G. R.; Horváth, I. T. Catalytic conversion of fructose, glucose, and sucrose to 5-(hydroxymethyl)furfural and levulinic and formic acids in  $\gamma$ -valerolactone as a green solvent. *ACS Catal.* **2014**, *4*, 1470–1477.
- (25) Garcés, D.; Díaz, E.; Ordóñez, S. Aqueous phase conversion of hexoses into 5-hydroxymethylfurfural and levulinic acid in the presence of hydrochloric acid: Mechanism and kinetics. *Ind. Eng. Chem. Res.* **2017**, *56*, 5221–5230.
- (26) Climent, M. J.; Corma, A.; Iborra, S. Conversion of biomass platform molecules into fuel additives and liquid hydrocarbon fuels. *Green Chem.* **2014**, *16*, 516–547.
- (27) Wang, X. Y.; Rinaldi, R. A route for lignin and bio-oil Conversion: Dehydroxylation of phenols into arenes by catalytic tandem reactions. *Angew. Chem. Int. Ed.* **2013**, *52*, 11499–11503.
- (28) Wang, X. Y.; Rinaldi, R. Exploiting H-transfer reactions with RANEY® Ni for upgrade of phenolic and aromatic biorefinery feeds under unusual, low-severity conditions. *Energy Environ. Sci.* **2012**, *5*, 8244–8260.
- (29) Kennema, M.; de Castro, I. B. D.; Meemken, F.; Rinaldi, R. Liquid-phase H-transfer from 2-propanol to phenol on Raney Ni: Surface processes and inhibition. *ACS Catal.* **2017**, *7*, 2437–2445.
- (30) Shrotri, A.; Kobayashi, H.; Tanksale, A.; Fukuoka, A.; Beltramini, J. Transfer hydrogenation of cellulose-based oligomers over carbon-supported ruthenium catalyst in a fixed-bed reactor. *ChemCatChem* **2014**, *6*, 1349–1356.

- (31) Scholz, D.; Aellig, C.; Mondelli, C.; Pérez-Ramírez, J. Continuous transfer hydrogenation of sugars to alditols with bioderived donors over Cu–Ni–Al catalysts. *ChemCatChem* **2015**, *7*, 1551–1558.
- (32) Schuchardt, U., Gallo J. M. R. in R. Rinaldi (Ed.), *Catalytic Hydrogenation for Biomass Valorization*, Chapter 11: Hydrogenolysis of lignocellulosic biomass with carbon monoxide or formate in pressurized hot water, Royal Society of Chemistry, UK, **2014**, p. 245, DOI 10.1039/9781782620099-00242.
- (33) Kapu, N. S.; Yuan, Z.; Chang, X. F.; Beatson, R.; Martinez D. M.; Trajano, H. L. Insight into the evolution of the proton concentration during autohydrolysis and dilute-acid hydrolysis of hemicellulose. *Biotechnol. Biofuels* **2016**, *9*, 224–234.
- (34) de Castro, I. B. D.; Graça, I.; Rodríguez-García, L.; Kennema, M.; Rinaldi, R.; Meemken, F. Elucidating the reactivity of methoxyphenol positional isomers towards hydrogen-transfer reactions by ATR-IR spectroscopy of the liquid–solid interface of RANEY<sup>®</sup> Ni. *Catal. Sci. Technol.* **2018**, *8*, 3107–3114.
- (35) Calvaruso, G.; Burak, J.A.; Clough, M.T.; Kennema, M.; Meemken, F.; Rinaldi, R. On the reactivity of dihydro-*p*-coumaryl alcohol towards reductive processes catalyzed by Raney Nickel. *ChemCatChem* **2017**, *9*, 2627–2632.
- (36) Haq, S.; Love, J. G.; Sanders, H. E.; King, D. A. Adsorption and decomposition of formic acid on Ni{110}. *Surf. Sci.* **1995**, *325*, 230–242.
- (37) Luo, Q. Q.; Feng, G.; Beller ; Jiao, H. J. Formic acid dehydrogenation on Ni(111) and comparison with Pd(111) and Pt(111). *J. Phys. Chem. C* **2012**, *116*, 4149–4156.

- (38) Ferri, D.; Buergi, T.; Baiker, A. Probing catalytic solid-liquid interfaces by attenuated total reflection infrared spectroscopy: Adsorption of carboxylic acids on alumina and titania. *Helv. Chim. Acta* **2002**, *85*, 3639–3656.
- (39) Deacon, G. B.; Phillips, R. J. Relationships between the carbon-oxygen stretching frequencies of carboxylato complexes and the type of carboxylate coordination. *Coord. Chem. Rev.* **1980**, *33*, 227–250.
- (40) Rothe, J.; Hormes, J.; Schild, C.; Pennemann, B. X-Ray Absorption spectroscopy investigation of the activation process of Raney Nickel catalysts. *J. Catal.* **2000**, *191*, 294–300.
- (41) Watanabe, N.; Ramos, A. Y.; Ferreira, J. A. M.; Tolentino, H. C. N. XAS and XRD studies on the structural changes of Ni-Raney catalyst after a hydrogenation process. *Phys. Scr.* **2005**, *T115*, 727–728.
- (42) Bernskoetter, W. H.; Hazari, N. Reversible hydrogenation of carbon dioxide to formic acid and methanol: Lewis acid enhancement of base metal catalysts. *Acc. Chem. Res.* **2017**, *50*, 1049–1058.
- (43) Enthaler, S.; von Langermann, J.; Schmidt, T. Carbon dioxide and formic acid – the couple for environmental-friendly hydrogen storage? *Energy Environ. Sci.* **2010**, *3*, 1207–1217.
- (44) Graseman, M.; Laurency, G. Formic acid as a hydrogen source – recent developments and future trends. *Energy Environ. Sci.* **2012**, *5*, 8171–8181.
- (45) Joó, F. Breakthroughs in hydrogen storage – Formic acid as a sustainable storage material for hydrogen. *ChemSusChem* **2008**, *1*, 805–808.

- (46) Bircumshaw, L.L.; Edwards, J. The kinetics of the decomposition of nickel formate. *J. Chem. Soc.* **1950**, *0*, 1800–1809.
- (47) Dollimore, D. The production of metals and alloys by the decomposition of oxysalts. *Thermochimica Acta* **1991**, *177*, 59–75.
- (48) Fox, P. G.; Ehretsmann, J.; Brown, C. E. The development of internal structure during thermal decomposition: Nickel formate dihydrate. *J. Catal.* **1971**, *20*, 67–73.
- (49) Meemken, F.; Mueller, P.; Hungerbuehler, K.; Baiker, A. Simultaneous probing of bulk liquid phase and catalytic gas-liquid-solid interface under working conditions using attenuated total reflection infrared spectroscopy. *Rev. Sci. Instrum.* **2014**, *85*, 084101.
- (50) Cezar, J. C.; Souza-Neto, N. M.; Piamontese, C.; Tamura, E.; Garcia, F.; Carvalho, E. J.; Neueschwander, R. T.; Ramos, A. Y.; Tolentino, H. C. N.; Caneiro, A.; Massa, N. E.; Martinez-Lope, M. J.; Alonso, J.A.; Itiw, J.-P. Energy-dispersive X-ray absorption spectroscopy at LNLS: investigation on strongly correlated metal oxides. *J. Synchrotron Rad.* **2010**, *17*, 93-102.

## For Table of Contents Use Only



Hemicellulose acts as a direct and indirect source of carboxylic acids in lignin-first biorefining. In the lignin-first biorefining, the formation of formic acid is suppressed by hydrogenation of sugars to sugar alcohols.